

The Influence of Interreflections on Shape from Fluorescence

Irina-Mihaela Ciortan , Sony George , Jon Yngve Hardeberg ; Colourlab, Department of Computer Science, NTNU - Norwegian University of Science and Technology, Gjøvik, Norway

Abstract

Fluorescence is an optical phenomenon, specific to certain materials that absorb light with higher energy and re-emit it at lower energy, with unnoticeable time latency. Due to this so-called Stokes shift, fluorescent materials pose several challenges in image capture, where usually a filtering setup is required at the illumination and/or sensing ends. Nevertheless, fluorescence emission is diffuse, which was previously used in shape from photometry models. In this work, we target the shape from fluorescence method for a specific category of materials: those with overlapping reflectance and fluorescence signals. In particular, we investigate how the self-interreflections (light bounces off a surface that get re-reflected by the surface itself) change the appearance of scenes with such fluorescent materials and how this affects the shape estimation with a photometric stereo model. To avoid instrumental artifacts inherent in real image capture setups, we perform our analysis on a synthetic dataset of multi-light images, generated with a physically-based spectral renderer that supports fluorescence.

Introduction

Fluorescence is a widespread phenomenon, present in nature (take chlorophyll for instance), as well as in man made materials. In many cases, fluorescent materials have an attractive glowing appearance, as a result of the increased saturation and brightness that come with the re-emission of light. In other cases, fluorescence allows the embedding of certain hidden details that can only be revealed under specific illumination and viewing conditions. It is for this reason that artificial fluorescent materials were created for and used in many applications: brightening agents in paper and detergents, modern artworks, fashion and cosmetic industry, traffic signage, watermarks, security markers in banknotes, etc.

Beyond the purely aesthetic advantages, fluorescent materials were exploited in the computer vision field, for their diffuse property [1], which makes them ideal for the classic photometric stereo model [2]. In a classic photometric stereo application, the shape of an object is computed from few images that vary only in the direction of the incident light while assuming the object can be described by a Lambertian model. This means that given a specular surface, one could spray it uniformly with a fluorescent paint and achieve a highlight-free shape estimation, as was done by [3, 4]. In addition to specularities, if the fluorescent material reflects a separate spectral range than its re-emission spectrum, then it is also free from inter-reflections, which is another deviation from the Lambertian assumption.

While the diffuse property of fluorescence is mostly taken for granted, there are several works that argue for the weak directionality of various fluorescent materials [5, 6]. Our work follows this line of research where we analyze the behaviour of fluorescent

scene from a multi-light and multi-spectral image collection. In a previous work, Ciortan et al. [7] analyzed the shape from fluorescence performance from real multi-light image captures of two handmade green mockups with UV-induced green emission. The normal recovery was worse in the fluorescent mode than in the reflective mode. In the current study, we mimic the real acquisition setup in a spectral renderer that supports physically-based synthesis of fluorescence. Moreover, we toggle on and off the indirect light effects and assess the performance of shape estimation in each case.

Therefore, our work has two main contributions. The first one consists in the simulation of a virtual multi-light and multi-spectral image collection setup of fluorescent scenes. This forms a dataset of multi-spectral multi-light image collections of fluorescent objects. While there exist such datasets for non-fluorescent objects [8], this is the first one for fluorescent scenes, to the best of our knowledge. The second contribution is given by an assessment of the impact of interreflections in shape estimation for objects made of materials that reflect the same wavelengths they fluoresce. When such materials emit fluorescence in the daylight, they are referred to as dayglo.

Related works

Fluorescence Rendering. In a fully physical characterization, fluorescent materials are best described by the bispectral bidirectional distribution and re-radiation function [5]. However, for rendering, as for shape estimation, simplifications are often done based on the Lambertian properties of fluorescence. Tominaga et al. [1] modelled the bispectral bidirectional radiance factor of a fluorescent object using a compact mathematical model based on the Lambertian behaviour for the fluorescent radiance factor and splitting the reflection into diffuse and specular reflection components. In a later work, Tominaga et al. [9] proposed a decomposition of spectral images of fluorescent objects with known geometry and bispectral matrix, into five basis factors, which were afterwards coupled with Mitsuba spectral renderer [10].

Mojzík et al. [11] perfected a research-centered spectral renderer, Advanced Rendering Toolkit (ART) [12], to support the fully spectral rendering of bispectral materials, using path tracing and Hero wavelength sampling.

Shape from Fluorescence. Treibitz et al. [3] and Sato et al. [13] were the first to exploit the isotropic emission of fluorescence for improving the shape estimation with the photometric stereo model for objects that are specular in the reflective mode. Their method works for uniformly colored albedo and was validated for natural and artificial fluorescent objects. However, they do not explore the cases where the reflectance of an object overlaps with its fluorescence emission spectrum, which triggers self-

interreflections given a concavity. It is speculated that for these specific situations, the quality of the shape estimation will worsen. This is indeed exemplified by Fu et al. [4] who capture a V-shaped object that reflects the same wavelengths it fluoresces. They show that indeed, the shape estimation is worse in the fluorescent mode than in the reflective mode. They correct this with an analytical method to remove global illumination effects that emerges from the difference in albedo between the fluorescent and reflective scene. Similar to [3, 13], Salvant et al. [14] capture multi-light images in the fluorescent mode to detect aging artifacts in Georgia O’Keefe’s paintings.

Ciortan et al. [7] captured multi-light images of two hand-crafted objects with heterogeneous fluorescent composition and a complex geometry with both concavities and convexities. They captured the objects in visible reflectance mode, as well as in UV-induced fluorescence mode. Then, they recovered the shape with four polynomial variations of the classic photometric stereo model and found that angular error between the estimated and original normal map was higher in the fluorescent case than in the visible reflectance one. We extend this work by performing a similar comparison, only this time, on synthetic data, where we can better separate the influence of interreflections.

The Influence of Interreflections. Since the pioneering work of Nayar et al. [15], it is a known fact that in a photometric stereo setting, interreflections lead to the reconstruction of a shallower shape than the reference, a so-called pseudo-surface. This is because the interreflections create higher brightness values in the concavities of the surface, which changes the photometry of the scene in a way that is not related to the direct, local illumination modeled by the traditional photometric stereo model. Langer [16] investigated the effect of interreflections on color appearance in the CIE $L^*a^*b^*$ space. The author proved that lightness and chroma undergo most changes, but only for materials that already have a medium to high lightness value (> 50). This implies that the hue is invariant to indirect illuminations effects. However, these two works were focused on non-fluorescent objects. Somewhat similar to [16], in our work we offer an analysis of the color changes triggered by interreflections in fluorescent scenes.

Fu et al. [4] studied the influence of self-interreflections in shape from fluorescence, for the materials with overlapping reflectance and fluorescent spectral distributions. They show that when fluorescence is activated, the shape recovered is shallower than otherwise. This study was carried out on color images of a real V-shaped object. As insight for their fluorescence rendering pipeline, Tominaga et al. [10] use the similarity of interreflections’ spatial distributions in-between the reflective and fluorescent modes.

Experimental Design

In this work, we analyze the influence of interreflections on shape reconstruction and color appearance for objects made of dayglo materials. In particular, we use the bispectral measurements of two post-its, displayed in Fig. 2. Then, we use two geometries: one of the handmade mockups scanned by Ciortan et al. [7] and a simple V-shaped object. We synthesize these two objects with different albedo variations based on the post-it materials (see Fig. 3 and 4) using ART spectral renderer [12]. More precisely, we choose the following albedo variations: plain non-fluorescent green using only the reflectance of the green post-it

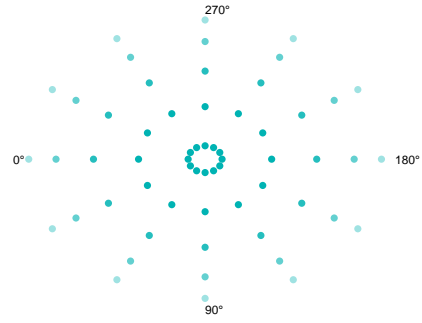


Figure 1. The light positions used for the rendered data.

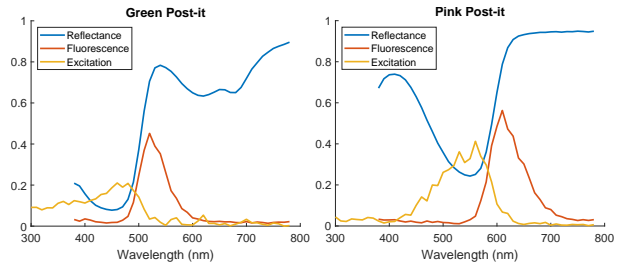


Figure 2. The two fluorescent materials included in our experiments.

(NF), uniform fluorescent green (G), fluorescent green with fluorescent pink stripes (GP). All the materials are synthesized as a Lambertian surface. Then, for the light distribution in the hemisphere, we sample the azimuth every 30 degrees $^\circ$, and at each azimuth location, we have 5 angles in the zenith, ranging from 25° to 85° with a step of 15° (see Fig. 1). For the V-shaped object, only the three innermost light rings were used (elevations 55° to 85°), because the others were impeding with the visibility of the scene. For each angular light direction, we render each scene twice: considering only the direct light effects (DL) and then activating the indirect light with 8 bounces (GI). To separate interreflections, we can make the difference between the two images, as showcased in Fig. 4.

In terms of spectral power distribution of the illumination, we use the CIE standard illuminant D65 and several synthetic illuminations that are step functions with cut-off at specific wavelengths. Accordingly, we selected a ultraviolet light - UV (cutoff after 390 nm), a visible light - VIS (cutoff below 520 nm) and a synthetic light to excite the fluorescence of the green post-it material (unit emission between 450 and 480 nm, centered at 465 nm, and zero emission elsewhere). Geometrically, all lights are mod-

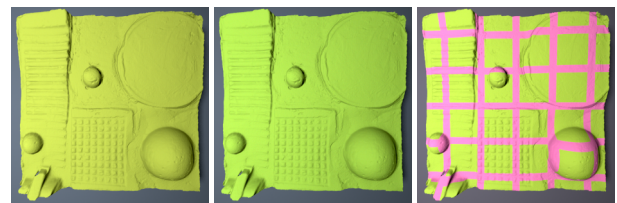


Figure 3. sRGB renderings of the mockup from [7] under D65 illuminant (direct light only), with different albedos: uniform non-fluorescent green, uniform fluorescent green, fluorescent green-pink stripes. Luminance was clipped where it exceeded the maximum value.

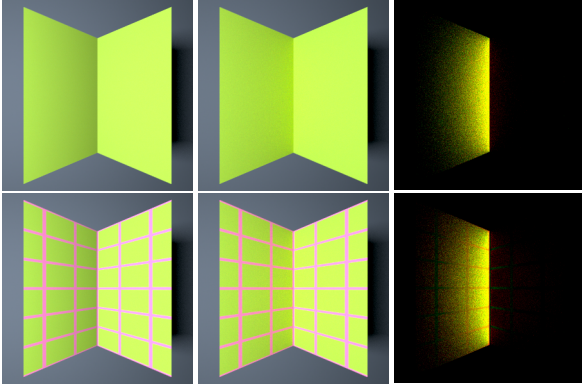


Figure 4. sRGB renderings of the V-shaped object under D65 illuminant, azimuth 0° , elevation 70° . Top: uniform fluorescent green albedo. Bottom: fluorescent green-pink stripes. Left: DL only. Middle: DL and GI. Right: Difference image that highlights the spatial extent of the interreflections (the contrast was increased here for visualization purposes).

elled as a planar area light source, and kept at a constant distance from the object at every angle.

Each rendered image has a spatial resolution of 512×512 pixels, and a multi-spectral representation of 8 bands that sample the visible range of the electromagnetic spectrum every 40 nm, from 380 to 700 nm. The multispectral images are then converted to color after a tone mapping operator is applied. The default tone mapping in ART is luminance clipping. However, we applied Reinhard02 [17], which was found to be the best tone mapping operator in most of the natural scenes as found by Cerda-Company et al. [18], although fluorescent objects were not specifically included in their study.

After rendering the multi-light and multi-spectral image collections for the various combinations of geometry, material and illuminant, we performed shape estimation on the Reinhard02 [17] tone mapped color images. The model we employed is the classic first-order polynomial representation of the photometric stereo model fitted with least-squares regression (PS-L2). As a form of quantitative comparison, we computed the angular error between the ground-truth and the estimated normal maps.

Results and Discussion

The results show that the normal reconstruction is affected by the presence of interreflections and this is especially obvious for the V-shape object where concavities are deeper than in the mockup geometry. At the same time, it appears that normal reconstruction is not affected when the object is made of a material with overlapping fluorescence and reflectance signals. Fig. 5 shows the distribution of angular errors between the reconstructed normal maps and the ground-truth for each studied geometry, while considering or not global illumination. Moreover, the results are plotted for the various albedos (uniform or with stripes) and illuminations, that activate or not the fluorescence.

The top boxplot in Fig. 5 depicts the angular errors for the mockup shape, for direct light only and global illumination included cases. We can see that the differences in albedo and illumination are less significant than the inclusion of interreflections. This means that for the mockup shape with a diffuse dayglo ma-

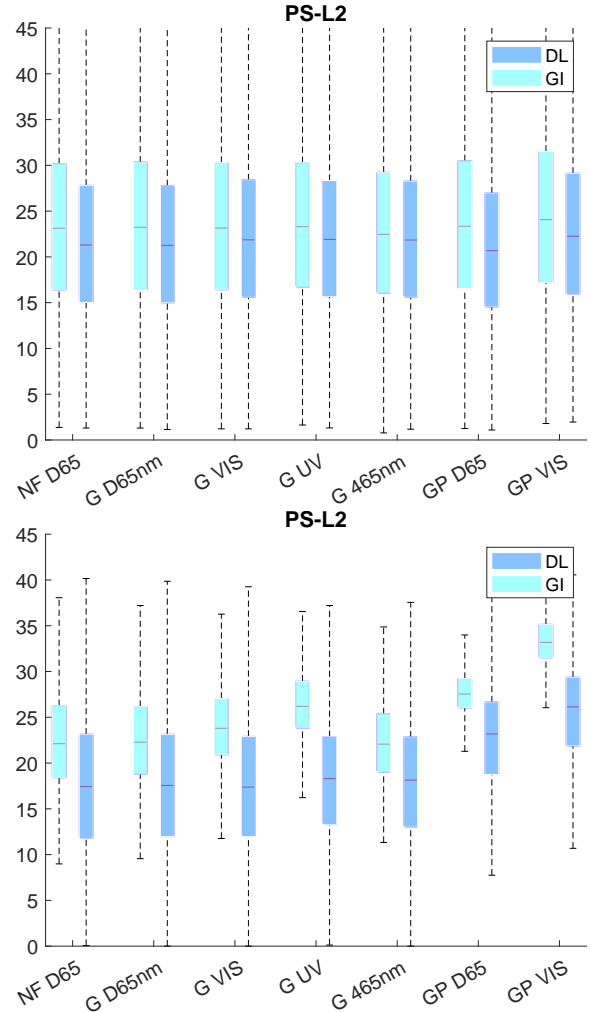


Figure 5. Angular errors wrt ground-truth for the normal maps recovered from the multi-light image collections of the mockup (top) and the V-shaped object (bottom). The main difference is triggered by the presence of inter-reflections.

terial, self-interreflections do not influence to a greater extent the shape recovery in the fluorescent mode than in the diffuse reflective mode.

Nonetheless, while the mockup has small concavities, because of the way it was manufactured, it contains other geometrical details as well. For this reason, we performed the same analysis on a V-shaped object with a 90° angle, where the concavity is deeper and the main feature of the geometry of the object. In this case, there is more variation in the angular errors (bottom boxplot in Fig 5) depending on the albedo. For example, the error is higher for the non-uniform albedo (green with pink stripes). The spatial representation of this angular error (Fig. 6) shows how the stripe pattern introduces variation, and how the insertion of interreflections leverages the magnitude of the errors around the concavity of the V-shape object. However, similar with the mockup shape, the error does not vary significantly when fluorescence is activated (G 465 nm) than when it is not (NF D65). This reinforces

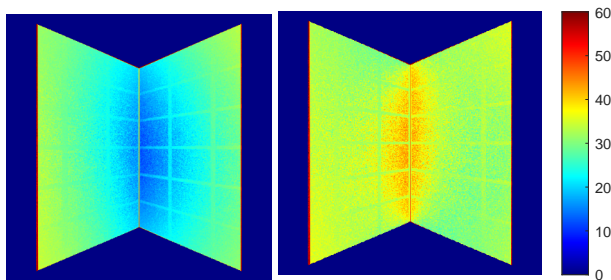


Figure 6. Per-pixel angular error for the normal reconstruction of the V-shape with fluorescent green-pink albedo, GP-VIS, under direct illumination only (left) and global illumination included (right). In the latter, the error increases around concavities, where there are more interreflections.

that self-interreflections do not pose a bigger challenge for dayglo materials than they do for plain reflective materials.

As a matter of fact, in the fluorescent-only mode, the overall light signal is lower than it is for the reflective signal. In Fig. 7, we show the difference between direct light and global illumination images at 520 nm, which is the peak of fluorescence emission for the green post-it, as well as high reflective band. Hence, it is a spectral band where self-interreflections are present. Nonetheless, the differences are lower for the fluorescent case than the reflective one. This is because the overall magnitude of the fluorescent emission is in itself lower in scale than reflectance, as it can be seen in Fig. 2. Then, interreflections further attenuate the original signal. If the original light signal is lower in the fluorescent case, the resulting bounced signal will be dimmer as well.

Although CIE $L^*a^*b^*$ and CIE LCh color spaces were not defined for fluorescent colors, we will use them to assess the difference determined by interreflections. Fig. 8 depicts the changes in chroma determined by global illumination effects for the V-shape rendered as NF D65 and as G 465 nm. In both cases, the difference attenuates with higher elevation angles. In addition, the level of difference is higher for fluorescent objects. As emerges from Fig. 9, the hue angle changes more for the fluorescent objects as well, albeit the very small amplitude of the change. Also, it seems that chroma changes to a higher extent than hue, which is in agreement with the study of Langer [16] performed on non-fluorescent objects only. Interestingly, there seems to be more variation with light direction for the ΔC^* and Δh° when compared with the changes at the single-wavelength case at 520 nm (Fig. 7). This hints that perhaps, visually, the effect of interreflections is more noticeable for fluorescent objects than it is for plain reflective ones. Nevertheless, the color appearance of fluorescent objects is an under-researched topic and further studies including psycho-physical experiments should be carried out to better understand how fluorescent objects with different geometries and spectral properties are perceived by human observers.

Conclusion

In this article, we analyzed whether interreflections represent a major drawback for the photometric stereo solution to shape reconstruction for fluorescent objects. To this purpose, we rendered multispectral multi-light image collections of two shapes covered with dayglo materials that reflect and fluoresce in the same spectral range.

Our results show that indeed, interreflections affect shape estimation, but in a similar way for both fluorescent and diffuse reflective objects. This is somewhat counter-intuitive after the results in [7], but we have to consider that there are still many discrepancies between the rendered and captured data. To begin with, the composition of the real mockup is more heterogeneous and the content of fluorophores is not uniform. Then, the real imaging setup is based on a trichromatic camera with filters attached and active illumination control to exclude/include fluorescence. Moreover, the captured data is influenced by the signal-to-noise ratio, which is not considered in the simulation.

In addition, through the color analysis in the current article we found that chroma and hue change to a higher extent for fluorescent objects than for diffuse reflective objects, when self-interreflections are present.

References

- [1] Shoji Tominaga, Keita Hirai, and Takahiko Horiuchi, “Measurement and modeling of bidirectional characteristics of fluorescent objects,” in *Image and Signal Processing: 6th International Conference, ICISP 2014, Cherbourg, France, June 30–July 2, 2014. Proceedings 6*. Springer, 2014, pp. 35–42.
- [2] Robert J Woodham, “Photometric stereo: A reflectance map technique for determining surface orientation from image intensity,” in *Image Understanding Systems and Industrial Applications I*. International Society for Optics and Photonics, 1979, vol. 155, pp. 136–143.
- [3] Tali Treibitz, Zak Murez, B. Greg Mitchell, and David Kriegman, “Shape from Fluorescence,” in *Computer Vision – ECCV 2012*, Andrew Fitzgibbon, Svetlana Lazebnik, Pietro Perona, Yoichi Sato, and Cordelia Schmid, Eds., Berlin, Heidelberg, 2012, Lecture Notes in Computer Science, pp. 292–306, Springer.
- [4] Ying Fu, Antony Lam, Yasuyuki Matsushita, Imari Sato, and Yoichi Sato, “Interreflection removal using fluorescence,” in *European Conference on Computer Vision*. 2014, pp. 203–217, Springer.
- [5] Matthias B. Hullin, Johannes Hanika, Boris Ajdin, Hans-Peter Seidel, Jan Kautz, and Hendrik P. A. Lensch, “Acquisition and analysis of bispectral bidirectional reflectance and radiance distribution functions,” in *ACM SIGGRAPH 2010 papers*, New York, NY, USA, Jul 2010, SIGGRAPH ’10, p. 1–7, Association for Computing Machinery.
- [6] Silja Holopainen, Farshid Manoocheri, and Erkki Ikonen, “Goniofluorometer for characterization of fluorescent materials,” *Applied Optics*, vol. 47, no. 6, pp. 835–842, Feb 2008.
- [7] Irina-Mihaela Ciortan, Andrea Giachetti, Sony George, and Jon Yngve Hardeberg, “Fluorescence transformation imaging,” in *Optics for Arts, Architecture, and Archaeology VIII*. Jun 2021, vol. 11784, p. 156–172, SPIE.
- [8] Boxin Shi, Zhipeng Mo, Zhe Wu, Dinglong Duan, Sai-Kit Yeung, and Ping Tan, “A benchmark dataset and evaluation for non-lambertian and uncalibrated photometric stereo,” *IEEE transactions on pattern analysis and machine intelligence*, vol. 41, no. 2, pp. 271–284, Feb 2019.
- [9] Shoji Tominaga, Keita Hirai, and Takahiko Horiuchi, “Appearance reconstruction of mutual illumination effect be-

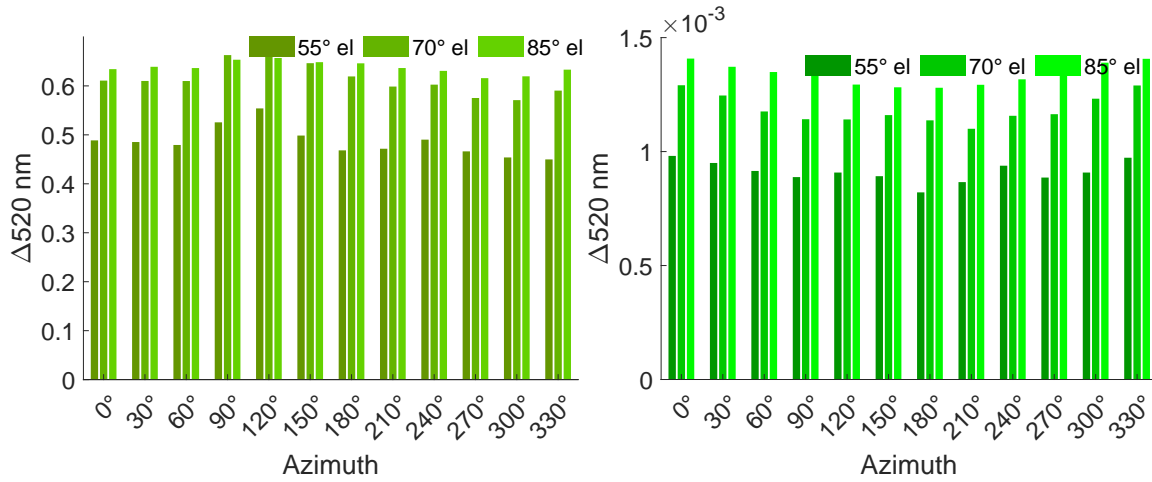


Figure 7. The effect of self-interreflections, plotted as maximum difference between DL and GI at 520 nm (peak of fluorescence of the green post-it, that overlaps with its reflectance), for the V-shape with plain green albedo rendered under D65, NF D65 (left), and green fluorescent albedo rendered under the excitation light, G 465 nm (right). Notwithstanding the distinct orders of magnitude, the proportionality of the difference with elevation angle is similar in both cases.

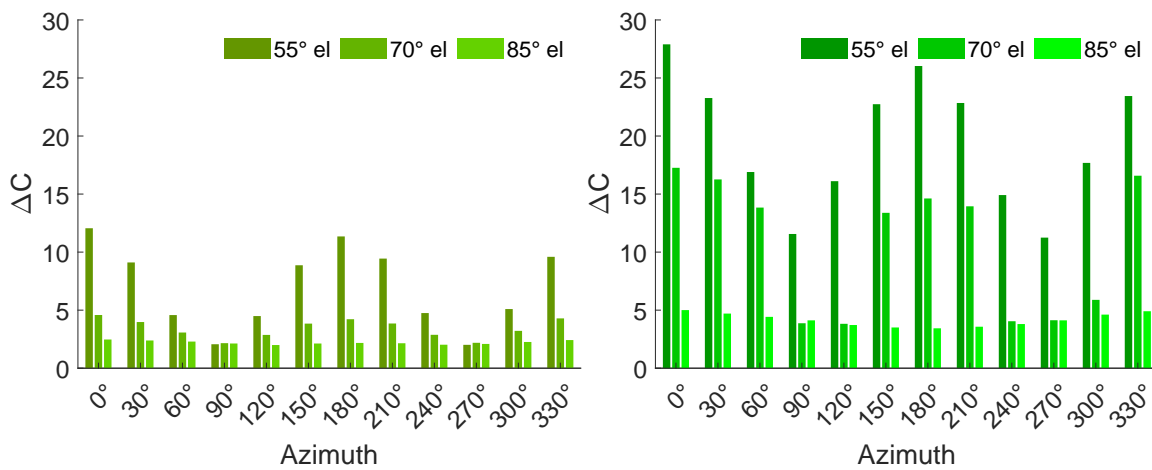


Figure 8. The effect of interreflections on C^* , plotted as maximum difference of C^* at each light position, between DL and GI for the V-shape with plain green albedo, NF D65 (left), and green fluorescent albedo rendered under the excitation light, G 465 nm (right). The overall magnitude of difference is higher in the fluorescent case. The difference decreases with light elevation angle.

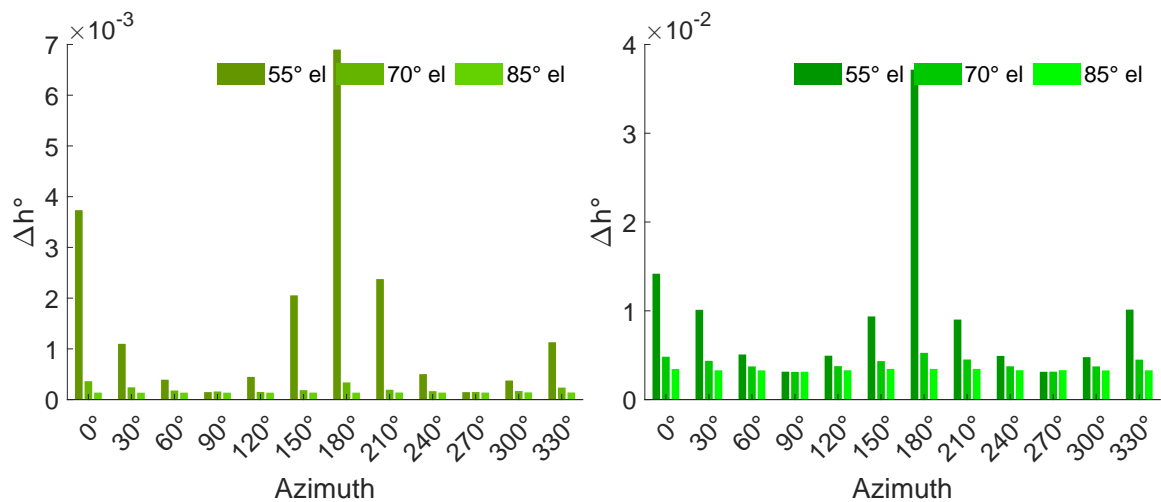


Figure 9. The effect of interreflections on h^r , plotted as maximum difference of h^r at each light position, between DL and GI for the V-shape with plain green albedo, NF D65 (left), and green fluorescent albedo, G 465 nm (right). The high values at 0° and 180° azimuth are probably due to the raking light effects coinciding with the sides of the V.

tween plane and curved fluorescent objects,” *Electronic Imaging*, vol. 2019, no. 6, pp. 485–1, 2019.

- [10] Shoji Tominaga and Giuseppe Guarnera, “Appearance synthesis of fluorescent objects with mutual illumination effects,” *Color Research & Application*, Oct. 2021.
- [11] M. Mojzík, A. Fichet, and A. Wilkie, “Handling fluorescence in a uni-directional spectral path tracer,” *Computer Graphics Forum*, vol. 37, no. 4, pp. 77–94, Jul 2018.
- [12] “Advanced Rendering Toolkit - physically based rendering taken a step further,” (Accessed on 2023-02-02).
- [13] I. Sato, T. Okabe, and Y. Sato, “Bispectral photometric stereo based on fluorescence,” in *2012 IEEE Conference on Computer Vision and Pattern Recognition*, June 2012, pp. 270–277, ISSN: 1063-6919.
- [14] Johanna Salvant, Marc Walton, Dale Kronkright, Chia-Kai Yeh, Fengqiang Li, Oliver Cossairt, and Aggelos K. Katsaggelos, “Photometric Stereo by UV-Induced Fluorescence to Detect Protrusions on Georgia O’Keeffe’s Paintings,” in *Metal Soaps in Art: Conservation and Research*, Francesca Casadio, Katrien Keune, Petria Noble, Annelies Van Loon, Ella Hendriks, Silvia A. Centeno, and Gillian Osmond, Eds., Cultural Heritage Science, pp. 375–391. Springer International Publishing, Cham, 2019.
- [15] Shree K Nayar, Katsushi Ikeuchi, and Takeo Kanade, “Shape from interreflections,” *International Journal of Computer Vision*, vol. 6, no. 3, pp. 173–195, 1991.
- [16] Michael S. Langer, “A model of how interreflections can affect color appearance,” *Color Research & Application*, vol. 26, no. S1, pp. S218–S221, Jan 2001.
- [17] Erik Reinhard, Michael Stark, Peter Shirley, and James Ferwerda, “Photographic tone reproduction for digital images,” in *Proceedings of the 29th annual conference on Computer graphics and interactive techniques*, 2002, pp. 267–276.
- [18] Xim Cerda-Company, C. Alejandro Parraga, and Xavier Otazu, “Which tone-mapping operator is the best? a comparative study of perceptual quality,” *JOSA A*, vol. 35, no. 4, pp. 626–638, Apr 2018.

Author Biography

Irina-Mihaela Ciortan is a Postdoctoral Researcher at the Colourlab, NTNU, where she previously completed a PhD degree in Computer Science (2023), with a thesis entitled “Spectral and Multi-light Imaging for Cultural Heritage: Material Analysis and Appearance Reconstruction”. Irina holds a joint MSc diploma in Spectral Science and Multimedia Techniques awarded by the 4-university Erasmus Mundus Consortium “Colour in Informatics and Media Technology” (2013) and a BSc in Computer Science issued by the Faculty of Cybernetics, Statistics and Informatics in Bucharest, Romania (2011).

Sony George is currently Associate Professor at the Colourlab, NTNU since 2017. Before joining NTNU, he has worked as a researcher at Gjøvik University College, Norway. Sony obtained a PhD in Photonics from the Cochin University of Science and Technology, India in 2012. His research interests are in the field of colour imaging, spectral image processing, image quality, etc.

Jon Yngve Hardeberg received his MSc degree in signal processing from the Norwegian Institute of Technology in Trondheim, Norway in 1995, and his PhD from Ecole Nationale Supérieure des Télécommunications in Paris, France in 1999. After a short but extremely valuable industry career near Seattle, Washington, where he designed, implemented, and evaluated colour imaging system solutions for multifunction peripherals and other imaging devices and systems, he returned to academia and Norway in 2001. He is currently Professor of Colour Imaging at the Department of Computer Science at NTNU and member of the Colourlab.